

Research Article

Development, characterization & *in vitro* skin permeation of rutin ethosomes as a novel vesicular carrier

Anju Dhiman* and Deepika Singh

Department of Pharmaceutical Sciences, M.D. University, Rohtak-124001. Haryana, India

***Correspondence Info:**

Dr. (Mrs.) Anju Dhiman
Department of Pharmaceutical Sciences,
M.D. University, Rohtak-124001. Haryana, India
E-mail: ad_mdu@rediffmail.com

Abstract

Objective: The aim of the present study was to formulate and characterize rutin ethosomes and to evaluate the rutin ethosomes to enhance its skin permeation rate as compared to parent drug, rutin.

Materials and Methods: Rutin ethosomes were formulated by cold method and optimized using 2³ factorial design by design expert software (version 8.0). The optimized rutin ethosomes were characterized for particle size distribution, vesicular shape using scanning electron microscopy, zeta potential, entrapment efficiency and short term stability studies. A specially designed franz diffusion cell was used for the percutaneous absorption studies of optimized rutin ethosomes using pig ear skin and the results were analysed using DD solver 8 software.

Results and Discussion: The entrapment efficiency of optimized ethosomes prepared using phospholipid concentration of 2.5 g with 30 ml ethanol for 12.5 minutes, was found to be maximum i.e. 73.9 %. Lipid vesicular system of rutin exhibited a negative zeta potential of -46.0 mV indicating a high degree of stability for rutin ethosomes. *In vitro* drug permeation studies of pure rutin and rutin ethosomes suggested that rutin ethosomes were better able to permeate across pig ear skin at the end of 120 minutes than pure rutin. Therefore, rutin ethosomes were better able to facilitate permeation of rutin deeply into the pig ear skin when compared with pure rutin.

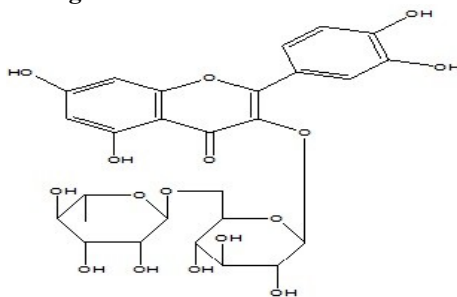
Conclusion: Rutin ethosomal formulation has tremendous potential to serve as a topical drug delivery system due to its enhanced rate of permeation.

Keywords: Ethosome, herbals, rutin, transdermal.

1. Introduction

Rutin also known as quercetin-3-rutinoside or sophorin is a flavonol glycoside comprised of the flavonol quercetin and the disaccharide rutinose (Figure 1). It is a polyphenolic compound widely distributed in higher plants. High concentrations of rutin are found in buckwheat seed, fruits and fruit rinds, especially in citrus fruits (e.g. orange, grapefruit, lemon etc). It has several pharmacological activities including anti-inflammatory¹, antioxidant², neuroprotective³, cardioprotective⁴, antiarthritis⁵ and psoriasis⁶. Rutin, a bioflavonoid has low solubility, less stability, low bioavailability and poor permeation⁷. In the present research study, rutin has been used for formulating a novel vesicular carrier in the form of rutin because rutin is reported to have good antioxidant property.

Fig. 1 Chemical structure of rutin



2. Materials and Methods

Phosphatidyl choline was purchased from Hi-media (Mumbai, India). Rutin was purchased from Loba Chemie (Mumbai, India). Ethanol was purchased from Central Drug House (Gujrat, India).

2.1 Experimental design: 2^3 full factorial design was used for process optimization of rutin ethosomes using design expert software (version 8.0).

2.2 Preparation of rutin ethosomes: The rutin ethosomes were prepared by cold method. In this method, phospholipid (2.5 g) was taken in a small round bottom flask and solubilized with 30 ml ethanol containing drug under mixing with a magnetic stirrer. The round bottom flask was covered to avoid ethanol evaporation. Distilled water was added slowly with continuous stirring to obtain the ethosome colloidal suspensions. The final suspension of ethosomes was kept at room temperature for 12.5 minutes under continuous stirring⁸.

2.3 Characterization of ethosomal system

2.3.1 Visualization by scanning electron microscopy (SEM): Visualization of rutin ethosomes was significantly achieved by scanning electron microscopy. Pure rutin and rutin ethosomes were mounted on a clear glass stub. It was then air dried and visualize under scanning electron microscope at X 10, 000 magnifications.

2.3.2 Measurement of ethosomal size distribution: The mean diameter of rutin ethosomes, soon after preparation and storage at $4 \pm 2^\circ\text{C}$ was determined by Zetasizer Nano ZS (Malvern, UK). Each sample was diluted using deionized water and the particle size distribution was determined.

2.3.3 Measurement of zeta potential: Zeta potential is the electrical potential of the vesicles, including its ionic atmosphere⁹. The zeta potential of the optimized rutin ethosomes was determined in distilled water at 20°C using Zetasizer Nano ZS (Malvern, UK).

2.3.4 Phospholipid – ethanol interaction: Phospholipid – ethanol interaction was assessed by $^1\text{H-NMR}$ using dimethylsulphoxide as solvent and by infrared spectroscopy (Perkin Elmer FTIR spectrophotometer, USA).

2.3.5 Transition temperature: Transition temperature was determined by Mettler-Toledo DSC (Columbus) instrument. The samples, pure rutin and rutin ethosomes were placed in aluminium pans and crimped followed by heating under nitrogen flow. Aluminium pan containing same quantity of indium was used as reference. DSC scans for rutin and rutin ethosome were recorded at heating rate of $10^\circ\text{C}/\text{minutes}$ at a temperature range of $10^\circ\text{C}- 300^\circ\text{C}$.

2.3.6 Entrapment efficiency: The entrapment efficiency of rutin in rutin ethosomes was estimated by ultra centrifugation technique. The total volume of the ethosomal preparation was measured and 2 ml of the formulation was transferred to a 10 ml glass centrifuge tube. The preparation was diluted with distilled water up to 5 ml and centrifuged at 2,000 rpm for 20 minutes using a cooling centrifuge (C-24 BL; Remi Instruments Ltd., Vasai, India) so as to separate out undissolved drug in the formulation. Ethosomes were separated by ultra centrifugation at 2,000 rpm for 20 minutes. Supernatant and sediment were recovered and their volume was measured. Following centrifugation, supernatant were separated from pellets and the amount of untrapped drug was measured spectrophotometrically at a wavelength 257 nm using UV visible spectrophotometer (Model- UV-2450, Shimadzu Corp., Kyoto, Japan). UV calibration curve of rutin obtained was: $y = 0016x + 0.009$ where y is rutin concentration and x is the absorbance, with R^2 value of 0.98. The amount of rutin entrapped in the ethosomal formulation was measured as the amount of rutin added during the preparation and its amount recovered in

the supernatant.

The entrapment efficiency was determined using the equation (i)

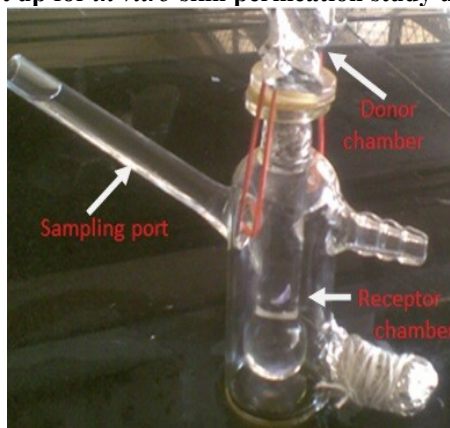
$$\text{Entrapment efficiency} = \frac{DE}{DT} \times 100 \dots\dots\dots(i)$$

where, DE is the amount of drug in the ethosomal sediment

and DT is a theoretical amount of drug used to prepare the formulation

2.3.7 In vitro skin permeation study: The pig ear skin was removed carefully from the pig’s ear obtained from local abattoir located in Jaipur city. The fat adhered to the dermis side was removed using a scalpel and isopropyl alcohol. The excised skin was washed with tap water and then phosphate-buffer saline (pH 7.4) dried and placed on aluminium foil, stored in refrigerator and used within two days. The *in vitro* skin permeation study of rutin ethosome and pure rutin from different formulations was studied using a specially designed franz glass diffusion cell with effective permeation area of 3.14 cm² and receptor cell volume of 11 ml as shown in Figure 2. The temperature was maintained at 37 ± 0.5°C. The receptor compartment contained phosphate buffer saline (11ml). Excised pig ear skin was mounted between the donor and the receptor compartment. 3ml of formulation was placed in the donor compartment. Entire assembly was kept under stirring using magnetic stirrer. Samples were withdrawn from the receiver compartment at regular intervals for 120 min and analyzed spectrophotometrically at 257 nm. Same procedure was repeated using rutin ethosomes as a carrier system. The results were analysed using DD solver 8 software.

Fig. 2 Experimental set up for *in vitro* skin permeation study using franz diffusion cell



2.3.8 Stability study: Optimized rutin ethosomal formulation was stored at 4°C ± 2°C, 25°C ± 2°C/60 ± 5 % RH and 40°C ± 2°C/70 ± 5 % RH for one month and monitored for drug entrapment efficiency, colour change and sedimentation, if any.

3. Results

3.1 Scanning electron microscopy (SEM): The scanning electron micrographs showed that pure rutin exists in the form of acicular crystals while rutin ethosomes possess a closed spherical shape with rough surface morphology as shown in Figure 3 (a) and 3 (b) respectively.

Fig. 3(a) SEM of pure rutin

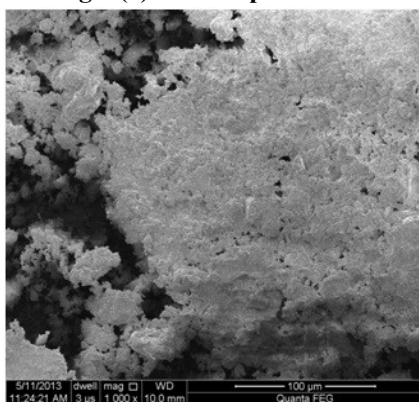
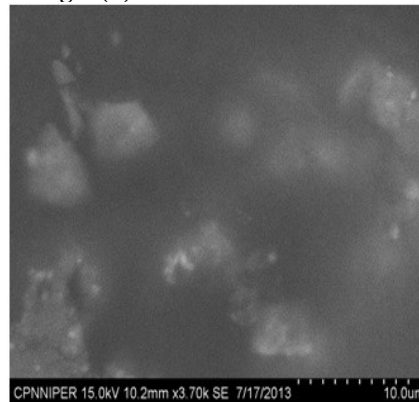


Fig. 3(b) SEM of rutin ethosome



3.2 Particle size distribution: Particle size and size distribution analysis of rutin ethosomes showed a narrow peak confirming the homogeneous population of the vesicular size. The average size values of rutin ethosomes was 642 nm and pure rutin was 21.23 μm as shown in Figure 4 (a) and 4 (b).

Fig. 4(a) Particle size and size distribution of rutin

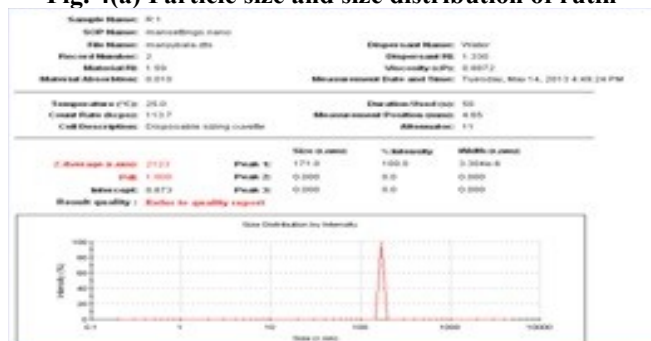
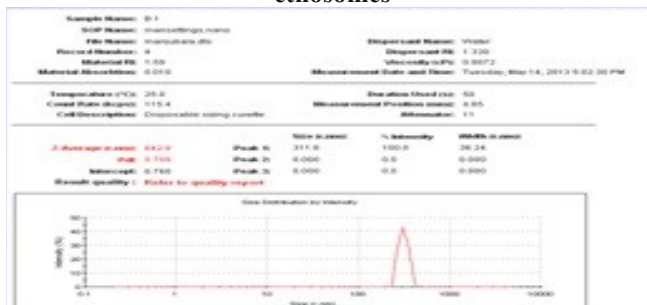
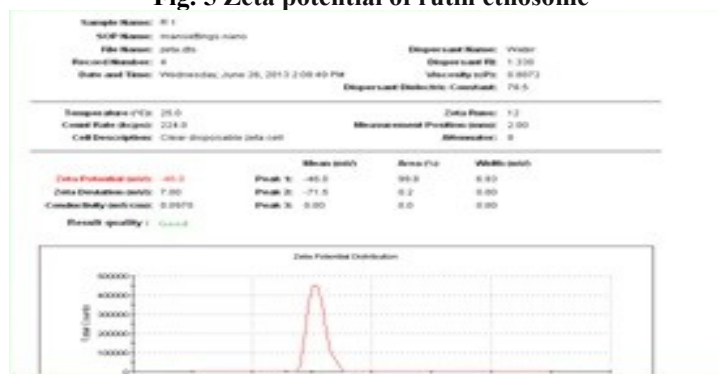


Fig. 4(b) Particle size and size distribution of rutin ethosomes



3.3 Zeta potential: The surface-charge properties of rutin ethosomes were investigated and results showed that rutin ethosomes formulation had negative charges on their surfaces with Z-potential value -46.0 mV (Figure 5). The Z-potential findings also highlighted a good degree of stability for ethosomes.

Fig. 5 Zeta potential of rutin ethosome



3.4 Entrapment efficiency: The various formulation composition consisted of total of eight runs according to 2^3 factorial design. The observed entrapment efficiencies of all the eight batches are tabulated in Table 1. The entrapment efficiency results for all the eight experimental combinations were fed into the design expert software to get optimized value for the variable parameters v.i.z. phospholipid concentration (g), time (min) and ethanol (ml) as shown. The entrapment efficiency of rutin ethosomes with BHT was 73.9 % for optimized batch.

The contour plot of optimization of rutin ethosomes for determination of phospholipid concentration, time and ethanol as process parameters is shown in Figure 6 (a). Three - dimensional plot representing the optimized values of phospholipid concentration and time at lowest standard error of design is shown in Figure 6 (b).

Table 1. 2^3 factorial design matrix of rutin ethosomes

Experiment	Phospholipid (g)	Time (min)	Ethanol (ml)	Entrapment efficiency (%)
1.	1	15	50	70.60 \pm 9.80
2.	1	10	10	19.25 \pm 4.55
3.	4	10	10	69.70 \pm 4.44
4.	4	10	50	19.85 \pm 4.47
5.	4	15	10	70.53 \pm 4.54
6.	1	15	10	25.35 \pm 3.97
7.	4	15	50	15.56 \pm 4.97
8.	1	10	50	68.60 \pm 4.30

Fig. 6(a) Contour plot of optimized rutin ethosome

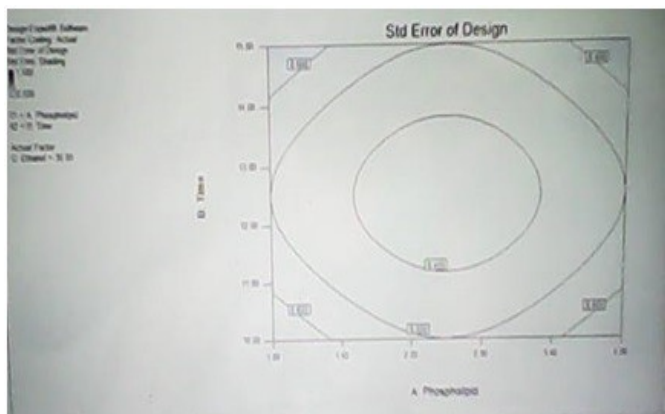
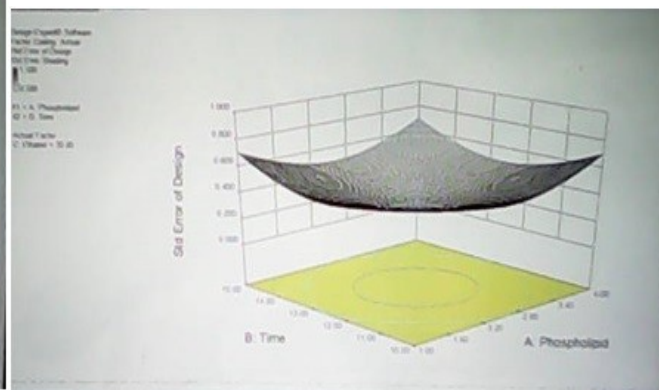


Fig. 6(b) Three-dimensional surface view of optimized rutin ethosomes



3.5 IR spectra: IR spectra of pure rutin and rutin ethosomes are shown in Figure 7(a) and 7(b) respectively. IR spectra of rutin showed peak at 1652 cm^{-1} including C=O stretching, aryl ketone), 1503 cm^{-1} including C=C stretching, for phenyl group and bending at 1202 cm^{-1} . A peak representing O-H functional group also appeared at 1313 cm^{-1} . Other characteristic peak observed was at 1059 cm^{-1} including C-O-C asymmetric stretching for ether and at 2938 cm^{-1} due to alkane (CH_3 asymmetric stretching). IR spectra of rutin ethosomes showed a peak at 1044 cm^{-1} representing C-O-C asymmetric stretching for ether group and at 1381 cm^{-1} which corresponds to -OH stretching. The peak at 1647 cm^{-1} (C=O stretching for aryl ketone) and at 2974 cm^{-1} due to alkane (CH_3 asymmetric stretching).

Fig. 7 (a) IR spectra of pure rutin

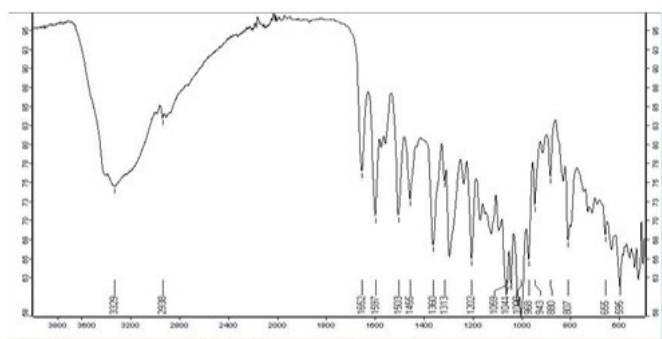
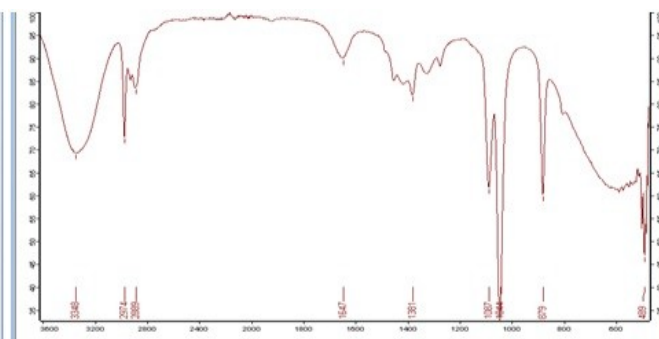


Fig. 7 (b) IR of spectra of rutin ethosomes



3.6 NMR spectra: NMR spectras of rutin and rutin ethosomes are shown in Figure 8 (a) and 8 (b) respectively. The spectra of rutin showed peaks at 6.184- 6.823 (m, 5H, Ar), 5.090 (s, 4H, OH), 5.292 (d, 1H, CH of tetrahydropyran), 4.371 (q, 1H, CH of tetrahydropyran), 3.42 (t, 1H, CH of tetrahydropyran) and 2.488 (s, 1H, OH of tetrahydropyran). However, NMR spectra of rutin ethosomes showed peak at 4.608 (q, 1H, CH of tetrahydropyran), 3.49 (t, 1H, CH of tetrahydropyran) and 1.046 (s, 3H, CH_3) indicating peak shift and changes in peak shape and peak position.

Fig. 8 (a) ^1H - NMR spectra of pure rutin

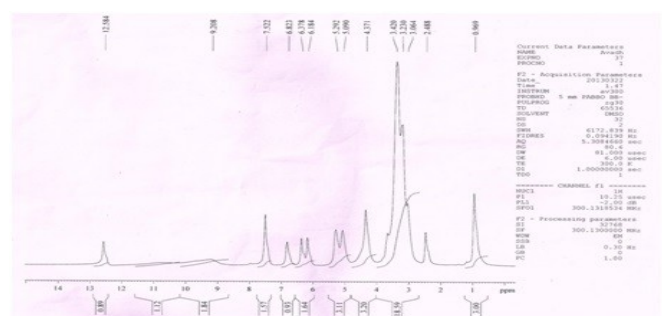
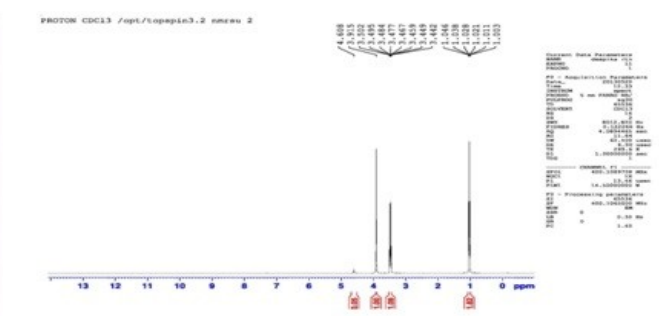


Fig. 8 (b) ^1H - NMR spectra of rutin ethosomes



3.7 Differential scanning calorimetry (DSC): The melting temperatures of the phospholipid in rutin ethosmes were evaluated by DSC as a parameter demonstrating the degree of phospholipid bilayers fluidity. As per DSC results, the melting point of rutin was found to be 157°C while rutin ethosmes melted at 145°C (Figure 9 (a) and 9 (b) respectively). DSC results indicated that the lipid bilayers in rutin ethosmes were in a fluid state, representing in a soft vesicular structure.

Fig. 9 (a) DSC thermogram of rutin

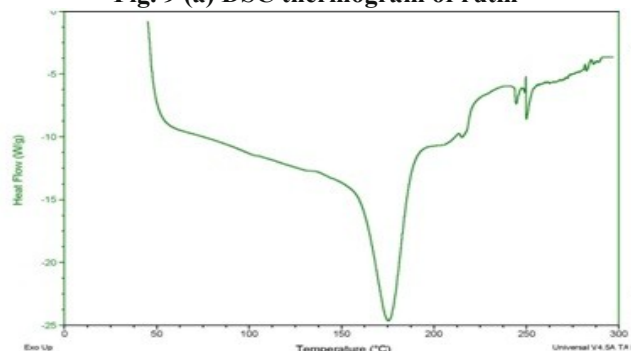
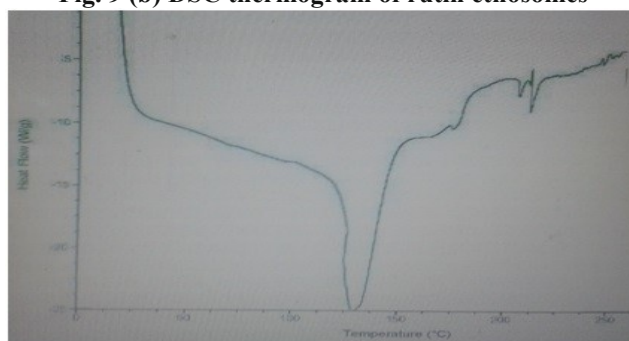


Fig. 9 (b) DSC thermogram of rutin ethosmes



3.8 In- vitro skin permeation study: Rutin ethosmes elicited an increased *in vitro* percutaneous permeation of rutin as compared with hydroalcoholic solution of rutin as shown in Figure 10.

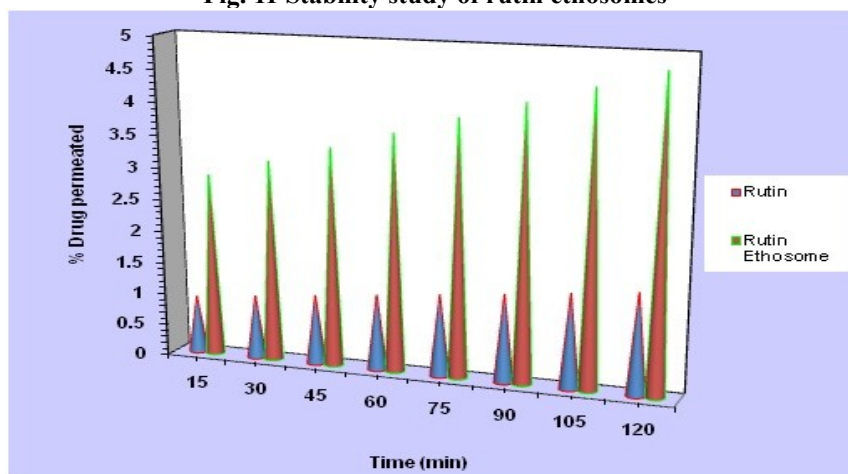
Fig.10 Comparison of *in vitro* skin permeation study of pure rutin and rutin ethosmes

3.9 Stability testing: The stability testing results of optimized rutin ethosomal formulation at different storage conditions are given in Table 2 and graph is shown in Figure 11. No change in colour and sedimentation was observed in optimized rutin ethosmes stored at 4°C and 25°C, however, slight colour change and sedimentation occurred in the optimized rutin ethosmes stored at high temperature i.e. 40°C at the end of 30th day.

Table 2. Stability study of rutin ethosmes

Time (days)	Percent entrapment (4°C ± 2°C)	Percent entrapment (25°C ± 2°C/60 ± 5 % RH)	Percent entrapment (40°C ± 2°C/70 ± 5 % RH)
0	73.9 %	73.9 %	73.9 %
5	73.9 %	73.84 %	70.34 %
10	73.88 %	73.75 %	68.98 %
15	72.3 %	69.70 %	66.6 %
20	70.86 %	68.70 %	63.6 %
25	70.76 %	67.72 %	62.72 %
30	69.3 %	66.3 %	59.35 %

Fig. 11 Stability study of rutin ethosmes



4. Discussion

In the present study, we investigated the *in vitro* skin permeation rate of a novel vesicular system of rutin in the form of rutin ethosomes. Rutin ethosomes were formulated by cold method and optimized using 2³ factorial design by design expert software (version 8.0). The physico-chemical properties of rutin ethosomes in terms of morphology, size, charge, phospholipid - ethanol interaction, transition temperature, entrapment efficiency, rate of skin permeation and stability w.r.t. particle aggregation/sedimentation and entrapment efficiency were studied.

Morphology study of rutin using SEM showed the existence of rutin as yellow coloured acicular crystalline powder with particle size of 21.23 µm. However, rutin ethosomes were amorphous in nature small in size (642 nm) and spherically symmetrical.

Zeta potential of rutin ethosomes showed negative values, which might be due to the nature of ethanol¹⁰. The zeta potential findings also highlighted a high degree of stability for ethosomes¹¹.

The negative value of surface charge is directly related to the size of rutin ethosomal vesicles that could be explained as a result of incorporation of high ethanol concentration. Probably, ethanol causes a modification of net charge of the system and confers it a good degree of stabilization that may finally lead to a decrease in the mean particle size of vesicles¹². DSC spectra of rutin ethosomes showed a decrease in transition temperature value of phospholipids which indicated that the ethosomal bilayers were in a more fluid state resulting in soft vesicular configuration¹³.

NMR and IR spectras of rutin ethosomes demonstrated the fluidizing effect of ethanol on the ethosomal phospholipid bilayers and confirmed phospholipid – ethanol interaction.

The optimized batch of rutin ethosomes showed the entrapment efficiency of 73.9 %. Higher entrapment efficiency of rutin in optimized rutin ethosomes could be inherent solubility of rutin in ethanol present in the ethosomal core and lipid bilayer. Moreover, the vesicles containing high ethanol concentration are reported to have thinner membranes, corresponding to the formation of a phase with interpenetrating hydrocarbon chains, which finally improved the entrapment efficiency of rutin ethosomes¹².

The hydroalcoholic solution of rutin was better able to facilitate penetration of rutin deeply into the pig ear skin, the amount delivered was only small relative to the delivery from the rutin ethosomal formulation. The optimized rutin ethosomes were better able to enhance penetration of a relatively large quantity of probe deeply into the skin.

The stability of ethosomal vesicles across time is a fundamental prerequisite to be investigated for their potential application as transdermal drug delivery system. In many cases, creaming, aggregation or sedimentation of ethosomal vesicles occurred during their storage and many components of the formulation are involved in this effect. For this reason, the physico-chemical stability of the rutin ethosomes was investigated¹⁴. Sedimentation was observed in optimized ethosomal formulation at the end of high temperatures storage conditions. Moreover, entrapment efficiency of rutin ethosome alter significantly after their storage for one months. At higher temperature, the decreased in entrapment efficiency, may be because of drug leakage¹⁵. The results of the present study demonstrated that rutin in the form of ethosomal vesicular system could improve the *in vitro* skin permeation of rutin and thereby can be used in therapeutics for variety of skin ailments.

5. Conclusion

Ethosomes have been considered as a possible vesicular carrier for transdermal delivery of rutin as an anti-inflammatory agent. The study confirmed that ethosomes of flavanoidal drugs are promising carrier for the transdermal delivery of parent drug (rutin, in this case). The enhanced accumulation of rutin via ethosomal carrier might help to optimize targeting this drug to the epidermal and dermal sites, thus creating new opportunities for modern topical application of rutin in the inflammatory conditions.

References

1. Hendra R, Ahmad S, Oskoueian E, Sukari A, Shukor M. Antioxidant, anti-inflammatory and cytotoxicity of *Phaleria macrocarpa* (Boerl.) Scheff Fruit. *BMC Complement Altern Med* 2011;11:1472-1482.
2. Lue B, Nielson N, Jacobsen C, Hellgren L, Guo Z, Xuebing X. Antioxidant properties of modified rutin esters by DPPH, reducing power, iron chelation and human low density lipoprotein assays. *Food Chem* 2010;123:221–230.

3. Javed H. Rutin prevent cognitive impairments by ameliorating oxidative stress and neuroinflammation in rat model of sporadic dementia of alzheimer type. *Neuroscience* 2012; 210:340-352.
4. Stanely P, Priya S. Preventive effects of rutin on lysosomal enzymes in isoproterenol induced cardiotoxic rats: Biochemical, histological and *in vitro* evidences. *Eur J Pharmacol* 2010;249:229-235.
5. Han Y. Rutin has therapeutic effect on septic arthritis caused by *Candida albicans*. *Int J Immunopharmacol* 2009;9:207–211.
6. Musthaba S, Athar M, Kamal T, Baboota S, Ali J, Ahmad S. Fast analysis and validation of rutin in anti-psoriatic ayurvedic formulation by HPLC. *J Liq Chromatogr Relat* 2011;34:446-455.
7. Vaishak M, Panday A. Assessment of flavonoid release with different permeation enhancers. *Int J Pharm Sci Res* 2012;4(2):154-156.
8. Touitou E, Dayan N, Bergelson L, Godin B, Eliaz M. Ethosomes- novel vesicular carriers for enhanced delivery: characterization and skin penetration properties. *J Control Release* 2000;65:403-418.
9. Li G, Fan C, Li X, Fan Y, Wang X, Mei Li, *et al*. Preparation and *in vitro* evaluation of tacrolimus-loaded ethosomes. *Sci World J* 2012:1-9.
10. Dave V, Kumar D, Lewis S, Paliwal S. Ethosome for enhanced transdermal drug delivery of aceclofenac. *Int J Drug Deliv* 2010;2:81-92.
11. Akhtar N, Pathak K. Cavamax w7 composite ethosomal gel of clotrimazole for improved topical delivery: development and comparison with ethosomal gel. *AAPS Pharm Sci Tech* 2011;13(1):344-355.
12. Zhou Y, Wei H, Zhang Q, Wu A. Synergistic penetration of ethosomes and lipophilic prodrug on the transdermal delivery of acyclovir. *Arch Pharm Res* 2010;33(4):567-574.
13. Godin B, Touitou E. Mechanism of bacitracin permeation enhancement through the skin and cellular membrane from an ethosomal carrier. *J Control Release* 2004;94:365-379.
14. Celia C, Cilurzo F, Trapasso E, Cosco D, Fresta M, Paolino D *et al*. Ethosomes and transfersomes containing linoleic acid: physicochemical and technological features of topical drug delivery carriers for the potential treatment of melasma disorders. *Biomed Microdevices* 2012;14:119–130.
15. Sathali A, Vijaykumar M, Arun K. Formulation and evaluation of diclofenac potassium ethosomes. *Indian J Pharm Sci* 2010;2(4):82-86.